

## Article

# The Influence of Initial Purity Level on the Refining Efficiency of Aluminum via Zone Refining

Xiaoxin Zhang <sup>1,2,†</sup>, Semiramis Friedrich <sup>2,\*</sup>, <sup>†</sup> and Bernd Friedrich <sup>2</sup> 

<sup>1</sup> State Key Laboratory of Advanced Special Steel, School of Materials Science and Engineering, Shanghai University, Shanghai 200444, China; zhangxiaoxin@shu.edu.cn

<sup>2</sup> IME Process Metallurgy and Metal Recycling, RWTH Aachen University, 52056 Aachen, Germany; BFriedrich@ime-aachen.de

\* Correspondence: SFriedrich@ime-aachen.de; Tel.: +49-241-80-95977

† These authors contributed equally to this work.

**Abstract:** Zone refining is a well-known technique, usually using pure initial materials to produce high purity metals. However, the effectiveness of zone refining in the purification of different purity levels of metals as well as its feasibility for use as a recycling technique for low quality metals are rarely investigated. In this work, conducted at IME/RWTH Aachen University, three kinds of Al with different purities, i.e., three-layer electrolysis (4N), commercial pure (2N8) and recycled Al (1N7), were put on focus to address the above-mentioned issue. The experiments were conducted with an optimized zone length combination at the moving rate of 1.2 mm/min for five zone passes. The results showed that the 4N pure initial Al was improved to 5N5 after five passes, much higher than the results for commercial pure- or recycled Al, where less than 50% reduction of total impurities was achieved.



**Citation:** Zhang, X.; Friedrich, S.; Friedrich, B. The Influence of Initial Purity Level on the Refining Efficiency of Aluminum via Zone Refining. *Metals* **2021**, *11*, 201. <https://doi.org/10.3390/met11020201>

Academic Editor: Mark E. Schlesinger  
Received: 7 December 2020  
Accepted: 18 January 2021  
Published: 22 January 2021

**Publisher's Note:** MDPI stays neutral with regard to jurisdictional claims in published maps and institutional affiliations.



**Copyright:** © 2021 by the authors. Licensee MDPI, Basel, Switzerland. This article is an open access article distributed under the terms and conditions of the Creative Commons Attribution (CC BY) license (<https://creativecommons.org/licenses/by/4.0/>).

**Keywords:** zone refining; aluminum; refining efficiency; purity level; initial concentration

## 1. Introduction

Zone refining is an effective methodology to produce high purity metals, which enables the distribution of impurities based on the principle of crystallization. As shown in Figure 1, it works by repeatedly moving one or a series of molten zones very slowly along a solid bar. Similar to other crystallization technologies, this process can be applied to refine any metals in which the distribution coefficients ( $k$ , the ratio of the concentration of an impurity in the solid phase to that in the liquid phase) of the impurities are smaller or bigger than unity. The bigger the difference from the unity  $k$  is, the higher the tendency of the impurities is to separate from the base metal. For example, the impurities of Fe, Cu, Ni, Ca, Ga, Ti, Si, Sb and Na in aluminum can be easily removed according to the values of their distribution coefficients in Table 1.

Zone refining has been applied for the production of highly pure metals such as from gallium [3], aluminum [4], up to tellurium [5], cadmium [6] and germanium [7] since the early 1950s [8]. A rule is that a high initial purity of the materials is already demanded. On one hand, the refining efficiency of one impurity usually increases with decreasing concentration [1,9]; on the other hand, purer raw materials lead to higher productivity and purity, which possess higher additional value and enable offsetting the drawbacks of the low production and high time-consumption. The commonly applied initial purity differs depending on type of metals treated and depends on the targeted final purity, as seen in Table 2. Lower purity metals such as commercial pure metals (cp) or secondary (recycled) metals are rarely purified by zone refining. However, it deserves a substantial attention nowadays under the circular economy targets. Therefore, a guideline towards the feasibility of zone refining is needed to purify the increasing volumes of secondary metals. In this paper, aluminum is closely brought into consideration to develop a rational

initial purity selection methodology based on the targeted purity for the future production process. The increasing application of high purity aluminum in high-tech areas, such as semiconductor, super conductor and capacitor foil, as well as the huge generation of Al waste, will lead to significantly varying purity levels. Additionally, this work explores the possibility of the removal of Fe from secondary Al through zone refining, as there is no effective method up to now for Fe removal from this Al-quality industrially.

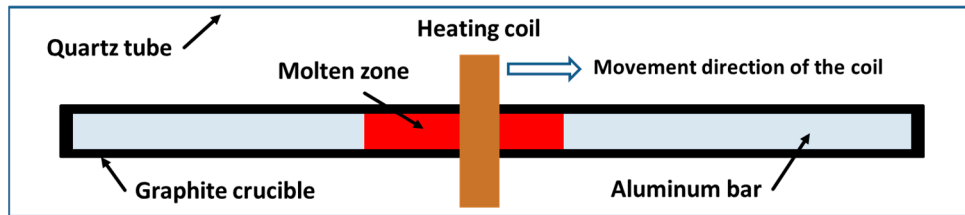


**Figure 1.** Diagram of zone refining of aluminum.

**Table 1.** Distribution coefficient ( $k$ ) of impurities in aluminum [1,2].

Element	Range of $k$	Element	Range of $k$
Ti	7–11	Cu	0.15–0.153
V	3.3–4.3	Si	0.082–0.12
Zr	2.3–3	Ga	0.11
Cr	1.8	Sb	0.09
Sc	0.9	Ni	0.004–0.09
Mn	0.55–0.9	Ca	0.006–0.08
K	0.56	Fe	0.018–0.053
Mg	0.29–0.5	Na	0.013
Zn	0.35–0.47	P	<0.01
Ag	0.2–0.3	Pb	0.0007
Au	0.18	-	-

**Table 2.** Exemplary high purity metals produced through zone refining shown with their initial and final purities.

Purity	Ga	Al	Ge	Te
Initial	4N6	5N2	5N	6N
Final	6N5 [10]	7N2 [11]	6N [12]	7N [4,13]

## 2. Experiments

The zone refining apparatus at IME/RWTH Aachen University with an inductive heater and an infrared camera (details presented in [16]) was utilized in this work, as shown in Figure 2. It is capable of generating up to 45 kW with a maximum frequency of 10 kHz. One-meter-long graphite crucible (ash content <200 ppm) was used simultaneously as the susceptor due to the weak inductive coupling between Al and the electromagnetic field. Three different purity-levels of aluminum, the product after three-layer electrolysis (4N), commercial pure (2N8) as well as a self-made secondary Al (1N7, from recycling of UBCs via salt bath smelting) were used as the starting point in this study, whose main compositions are presented in Table 3.

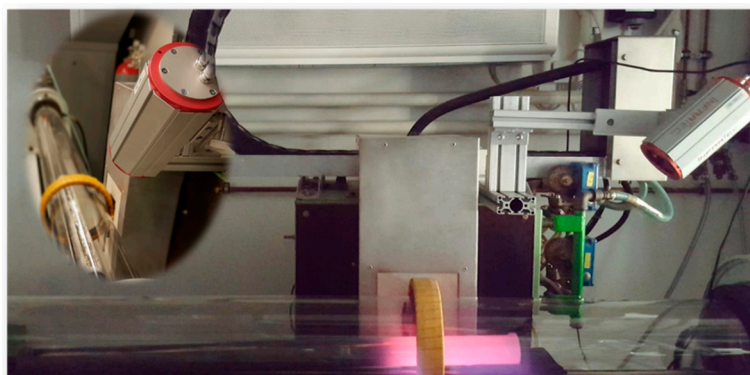


**Figure 2.** Zone refining device, equipped with an inductive heater and an infrared camera.

**Table 3.** Chemical composition of the different purity levels of Al, applied in this work (ppm).

Three-layer electrolysis Al <sup>1</sup>	Si	Na	Ti	Fe	Sn	Zn	Cu	P	Pb	Total impurities	Al (%)
	<5	18	9	<5	19	23	8	15	24	116	99.99
Commercial pure Al <sup>2</sup>	Fe	Ga	Ni	Si	Ti	V	-	-	-	Total impurities	Al (%)
	1450	77	35	354	26	51	-	-	-	1993	99.8
Recycled Al <sup>2</sup>	Si	Fe	Cu	Mn	Mg	Cr	Zn	Ti	Ga	Total impurities	Al (%)
	1790	4150	1500	8550	9900	140	310	180	90	26,610	97.3

Note: <sup>1</sup> analyzed by spark spectrometer, while, <sup>2</sup> analyzed by Inductively Coupled Plasma Optical Emission Spectrometer (ICP-OES), according to the required detection precision.

The feasibility of the zone length during the zone refining process has often been investigated, e.g., [10,17–21]. The latest result about the theoretical optimum zone length combination [10] based on the so called Spim model [17] was applied also in the present study. However, the real zone lengths deviated from the expected values, due to the limitation of the conditions of the used apparatus, by which the zone length is controlled by the inductive power and natural cooling. Table 4 shows the difference between the theoretical (calculated) and real (measured) zone lengths. The equipped single inductive heater could not realize the whole Al-bar in molten state, which was desired in the first pass based on the theoretical zone lengths scheme. Instead, the maximum of zone length achievable was around 35 cm (0.35 L, L represents the real length of the Al bar used in this work, 100 cm). Moreover, the zone length frequently varied even under the stable heater power and a constant heater movement velocity due to the high thermal conductive charge and crucible, leading the frequent failure of heat balance at the solid/liquid interface [6]. Therefore, a frequent adjustment of the power had to be carried out manually, according to the real zone length detected by an Infrared camera [16,22]. This allowed for a comparatively stable zone length as the heater moved. Nevertheless, the real zone length still varied to an extent of >20%, as seen in Table 4. A heater moving velocity of 1.2 mm/min was adopted in this study in view of the balance of high refining efficiency and low time-consumption in one single pass. A small tilting angle of 3–5° calculated based on the empirical equation [19] was set to suppress the commonly appeared mass transfer phenomenon during zone refining. Five passes were executed on each sample. The specimens of commercial pure and recycled Al bars after zone refining were taken every 10 cm (10% of total length) starting 2 cm from front edge after 1st, 3rd and 5th zone passes and were analyzed by ICP-OES. For the already 4N-pure Al, the impurity concentration after each zone pass was not determined by ICP-OES (detection limit of 10 ppm). Instead, only the bar after the fifth zone pass was analyzed by Glow Discharge Mass Spectrometry (GDMS), due to its higher precision and lower detection limit.

**Table 4.** Experimental parameters, applied on different initial purity levels.

Zone Pass	Optimum Zone Length [10]	Zone Length (Practical) *			Length of Al Bar (L)	Moving Velocity
		4N-Pure Al	2N8-Pure Al	1N7 Pure Al		
1st	1 L	0.24–0.34 L	0.17–0.36 L	0.23–0.32 L		
2nd	0.35 L	0.17–0.30 L	0.17–0.30 L	0.14–0.29 L		
3rd	0.25 L	0.17–0.28 L	0.20–0.30 L	0.20–0.30 L	100 cm	1.2 mm/min
4th	0.20 L	0.16–0.25 L	0.14–0.23 L	0.12–0.24 L		
5th	0.15 L	0.15–0.25 L	0.12–0.25 L	0.18–0.25 L		

Note: L represents the length of the Al bar; \* the practical zone length was measured by hand according to the clear interface between solid and liquid states of Al.

### 3. Results and Discussion

#### 3.1. Refining Efficiency of 4N Pure Al

The impurity concentrations along the bar after five passes are presented in Table 5. It shows that a purity of 5N5 could be achieved after five passes, manifesting the effectiveness of zone refining deployed to purify the 4N pure Al. Most of the impurities except for Na, Ti, Sn and Zn were significantly moved from the beginning to the end of the bar, resulting in a higher purity of Al at the beginning of the bar. The purity of Al in the impurity-enriched end (4N4) is strangely even higher than the initial purity of 4N (analyzed by spark spectrometer), which might be due to the difference of precision between these two analysis methods or the evaporation of some impurities with low vapor pressure, such as Na, Zn, P. The significant purification effect can be shown anyway by the clear impurity concentration gradients of the bar after refinement, as presented in Figure 3. The peak of the impurity level at 32 cm can be contributed to the high crystallization rate at this moment (this unstable crystallization effect was already addressed above).

**Table 5.** Impurity concentration along Al bar after five passes of zone refining with 4N pure Al as initial purity analyzed by GDMS (ppm).

Position (cm)	Si	Na	Ti	Fe	Sn	Zn	Cu	P	Pb	Total Impurities	Al (%)
Initial *	<5	18	9	<5	19	23	8	15	24	116	99.99
12	0.98	0.06	0.10	0.03	1.50	1.49	0.22	0.04	0.01	4.69	99.9995
32	2.05	0.15	0.25	3.45	0.04	20.95	1.62	0.09	1.09	29.86	99.997
52	1.49	0.12	0.15	1.45	0.08	1.32	1.21	0.07	0.44	6.34	99.9994
72	4.01	0.04	0.04	0.76	0.01	10.56	0.28	0.09	0.00	15.86	99.998
92	30.37	0.04	0.03	16.54	1.28	2.93	2.22	4.96	0.51	58.89	99.994

Note: \* it was analyzed by spark spectrometer.

#### 3.2. Refining Efficiency of 2N8 Pure Al

The average concentrations of impurities in the first half of the bar after each pass are presented in Table 6 (more detail of impurity concentration distribution after each pass can be seen in the Appendix A—Table A1). It shows that Si was significantly removed from the first half of the bar, while the reduction of Fe and Ni is lower. On the contrary, Ti and V were accumulated there due to their large distribution coefficients (see Table 1). The removal of Ga showed the biggest challenge amongst the whole impurities, only 26% removed after fifth pass, opposite to expectation due to the low value of k. In general, the reduction percentages of total impurities in the first half of the bar were 11%, 21% as well as 39% after 1st, 3rd and 5th zone passes respectively. Such levels of reduction are not sufficient enough in view of the cost of zone refining. Although the impurity concentrations in the cleanest parts (usually at the beginning of the bar) after each zone pass are much lower than the average in the first half of the bar, as seen in Table 7, the conclusion is the same in a general view.

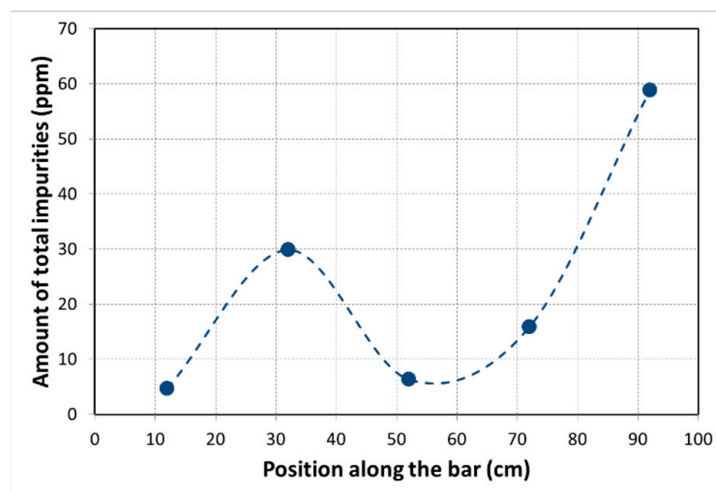


**Figure 3.** The distribution of the amount of all impurities along the Al bar after five zone passes using 4N pure Al as initial material.

**Table 6.** Impurity reduction in the first half of the bar after five passes of zone refining using 2N8 pure Al as initial material, analyzed through ICP-OES (ppm).

Impurity Elements	Fe	Si	Ga	V	Ni	Ti	Total Impurities
<b>Initial material</b>	1450	354	77	51	35	26	1993
<b>1st pass</b>	1300	222	89	86	30	40	1767
<b>3rd pass</b>	1200	151	75	86	23	40	1575
<b>5th pass</b>	900	86	57	100	18	50	1211
<b>Reduction (1st pass)</b>	10%	37%	−16%	−69%	14%	−54%	11%
<b>Reduction (3rd pass)</b>	17%	57%	3%	−69%	34%	−54%	21%
<b>Reduction (5th pass)</b>	38%	76%	26%	−96%	49%	−92%	39%

**Table 7.** Impurity concentration at the purest part of the bar after each pass of zone refining using 2N8 pure Al as initial material, analyzed through ICP-OES (ppm).

Impurity Elements	Fe	Si	Ga	V	Ni	Ti	Total Impurities
<b>Initial material</b>	1450	354	77	51	35	26	1993
<b>1st pass (at 32 cm)</b>	720	136	61	116	<10	66	1099
<b>3rd pass (at 52 cm)</b>	840	118	67	100	14	49	1188
<b>5th pass (at 12 cm)</b>	440	33	31	139	<10	88	731
<b>Reduction (1st pass)</b>	50%	62%	21%	−127%	>71%	−154%	44%
<b>Reduction (3rd pass)</b>	42%	67%	13%	−96%	60%	−88%	40%
<b>Reduction (5th pass)</b>	70%	91%	60%	−173%	>71%	−238%	63%

### 3.3. Refining Efficiency of Recycled Al (1N7)

The elements Mn and Mg represent the highest content as impurities in the recycled UBCs. The low reduction of these two elements—only 31% and 46% reduced after five passes—has limited the final purification effect, as seen in Tables 8 and 9. Low removing efficiency ( $\leq 50\%$  after five passes) was observed also for Si, Fe and Cu. Cr and Ti moved in the opposite direction to the heater because of their  $k$  higher than one. The average concentration of Ga in the first half of the bar and its concentration in the purest part are both unexpectedly higher than the initial concentration considering its  $k$  smaller than one. However, the decreasing tendency of its concentrations after each pass can demonstrate the removal effect it should have revealed after the first pass. The results also show that the existence of Ti, Cr and Ga would be detrimental when using zone refining to clean

recycling-pure aluminum. More data on impurity concentration distribution after each pass for zone refining of recycled Al can be seen in the Appendix A—Table A2.

**Table 8.** Impurity reduction in the first half of the bar after five passes of zone refining using 1N7 pure Al as initial material, analyzed through ICP-OES (ppm).

Impurity Elements	Mg	Mn	Fe	Si	Cu	Zn	Ti	Cr	Ga	Total Impurities
<b>Initial material</b>	9900	8550	4150	1790	1500	310	180	140	90	26,610
<b>1st pass</b>	7200	6100	3200	1000	1200	398	243	199	158	19,698
<b>3rd pass</b>	6100	6000	2400	700	900	302	301	203	137	17,043
<b>5th pass</b>	5300	5900	2100	900	800	248	349	210	130	15,937
<b>Reduction (1st pass)</b>	27%	29%	23%	44%	20%	−28%	−35%	−42%	−76%	26%
<b>Reduction (3rd pass)</b>	38%	30%	42%	61%	40%	3%	−67%	−45%	−52%	36%
<b>Reduction (5th pass)</b>	46%	31%	49%	50%	47%	20%	−94%	−50%	−44%	40%

**Table 9.** Impurity concentration at the purest part of the bar after each pass of zone using 1N7 pure Al as initial material, analyzed through ICP-OES (ppm).

Impurity Elements	Mg	Mn	Fe	Si	Cu	Zn	Ti	Cr	Ga	Total Impurities
<b>Initial material</b>	9900	8550	4150	1790	1500	310	180	140	90	26,610
<b>1st pass (at 42 cm)</b>	6600	6000	2700	820	1100	375	272	202	149	18,218
<b>3rd pass (at 22 cm)</b>	5400	5800	2000	470	800	297	405	212	129	15,513
<b>5th pass (at 2 cm)</b>	4400	5600	1400	710	620	261	694	227	119	14,031
<b>Reduction (1st pass)</b>	33%	30%	35%	54%	27%	−21%	−51%	−44%	−66%	32%
<b>Reduction (3rd pass)</b>	45%	32%	52%	74%	47%	4%	−125%	−51%	−43%	42%
<b>Reduction (5th pass)</b>	56%	35%	66%	60%	59%	16%	−286%	−62%	−32%	47%

As presented in Tables 8 and 9, the reduction percentage of the total impurities in the first half of the bar as well as in the purest part of the bar stepwise but slightly increases when the number of passes increases. However, only 40% and 47% of all impurities were removed in the first half of the bar and in the purest part of the bar respectively after five passes. This result implies a low economic situation to purify such recycling-level purity of Al with the purpose to produce significantly higher purity levels of the metal, using zone refining process. It proves however to be effective, if the target is just to reduce partly some certain impurities or some amounts of total impurities of the recycled aluminum. For example, Fe is the most troublesome impurity for the application of the secondary Al. The only way to reduce the amount of Fe to an accepted level in the industry is to dilute secondary Al in a raw pure Al, as there is no appropriate method to effectively remove Fe. However, zone refining showed a good separation effect for Fe, i.e., almost one fourth and half of Fe in the first half of the bar were separated after first and fifth pass respectively, as seen in Table 8.

#### 3.4. Comparison of Refining Efficiency among Zone Refining of Different Initial Purity-Levels of Al

Comparing the zone refining of 4N-, 2N8- as well as 1N7-Al (see Figure 4) showed that the reduction of impurity level in the first half of the bar for 4N-Al after fifth pass is much higher than that of the other two. Regarding to each zone refining pass, the reduction of impurity for 1N7-Al is more intensive in comparison to the case of 2N8-Al, but the slope of the trend-line is lower. The low reduction of all impurities in the first half of the bar for 2N8-Al in the first three passes originates from the insufficient refining efficiency of the main impurity Fe (i.e., 10% and 17% of reduction percentage after 1st and 3rd passes), as presented in Table 6. That could be due to the more unstable zone length appearing in the experiments, as seen in Table 4. Focusing on the purest part of the bar, the impurity

reduction percentage of 4N-Al is much higher than that of 2N8- and 1N7-Al, similar to the case of the first half of the bar, as seen in Figure 4. While, 2N8-Al shows a higher impurity reduction than the 1N7-Al, which is opposite to the case of the first half of the bar.

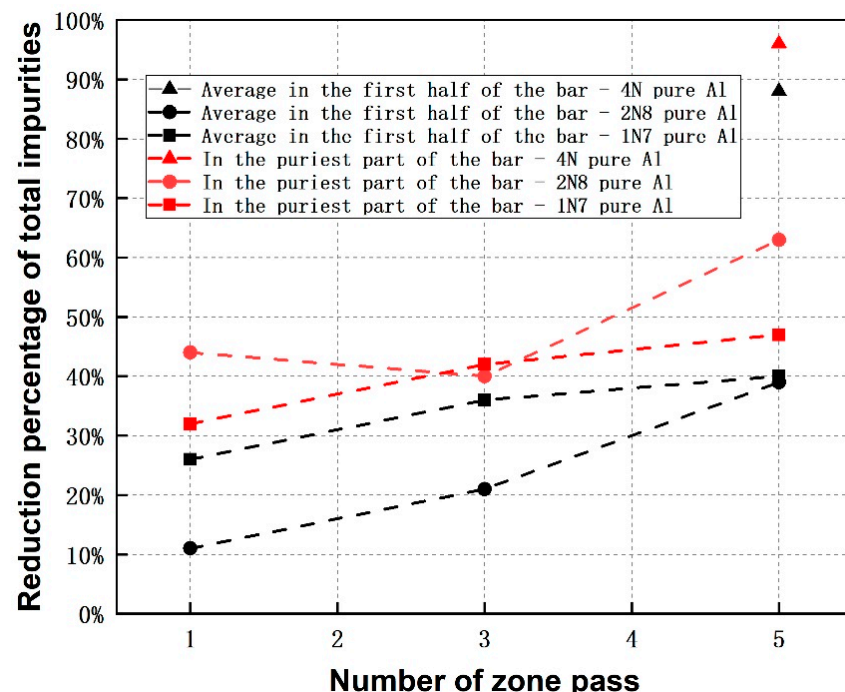


**Figure 4.** Comparison of reduction percentage of all impurities after each pass among zone refining of 4N-, 2N8- and 1N7 pure Al (the chemical composition of the Al after 1st and 3rd passes for zone refining of 4N pure Al were not analyzed in the present work, considering the huge probability of introducing contamination during sampling such high purity Al in the middle zone passes).

Overall and as a conclusion, the results indicate that if refined with a high number of zone passes ( $\geq 5$ ), the Al with a higher initial purity level has a higher refining efficiency regarding to the purest part of the bar or to the average values in the first half of the bar.

The impact of initial elementary concentration on the achievable refining efficiencies is hard to identify and therefore a safe conclusion cannot be drawn based on the present results. For example, Fe and Si show lower reduction efficiency in the first half of the bar in 2N8 pure Al compared to that in purified 1N7 pure Al, as seen in Figure 5a. It is opposite to the conclusion that the removal efficiencies of Fe and Si increase with their decreasing concentration, reported in reference [9]. Their refining efficiency in the purest part of the bar, however, seems not to have a relation to the initial concentrations, manifested in Figure 5b. The phenomenon is supposedly caused by the influence of the other co-existed impurities, which would affect the refining efficiency, through, e.g., forming an intermetallic compound or eutectic among them. Nevertheless, it can be found that the lower impurity concentration is favorable to obtain higher refining efficiency after increasing passes, e.g., the reduction percentage of Si in 2N8 pure Al after five passes is much higher than that in the recycled Al. This tendency was ascertained again by the extremely high refining efficiency of Fe or Si during the purification of 4N pure Al, as presented in Table 5.

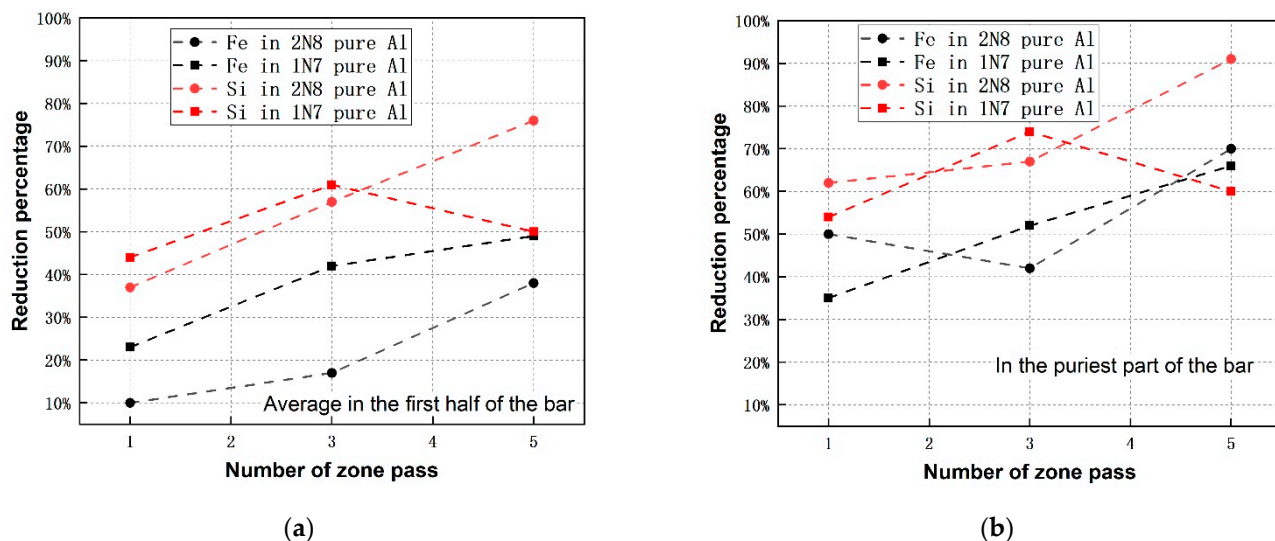


**Figure 5.** Comparison of remaining percentages of impurities Fe and Si after zone refining between commercial pure Al and recycled Al: (a) average in the first half of the bar; (b) in the purest part of the bar.

#### 4. Assessment and Conclusions

Aluminum with three different purity levels (4N (three-layer electrolysis Al), 2N8 (commercial pure Al) and 1N7 (recycled Al from UCBs)) was used to investigate the influence of initial purity of Al on zone refining efficiency (as example for crystallization methods) as well as to assess the feasibility of using this methodology to purify recycled Al especially regarding Fe. The results showed that Al with initial 4N purity had the highest refining efficiency of 96%, i.e., it was improved to 5N5 purity after five zone passes. However, the commercial pure- and recycled Al both showed impurity reduction percentage of less than 50%, measured in samples of the first half of the bar after five passes. The purification potential for these two Al raw materials is poor and do not allow considering commercial transfer, especially considering the low production yield and high time-consumption for zone refining.

Scientifically spoken, the correlation between the refining efficiency of each individual element (e.g., Fe and Si) could not be identified clearly in the conducted preliminary passes when observing the results of commercial pure and recycled Al. However, generally, an impurity with a lower initial concentration shows a higher potential to be removed (in terms of reduction percentage), but using high number of passes. The refining efficiency of the impurities with a very low concentration in 4N-pure Al was much higher than the refining efficiency of them in commercial pure and recycled Al, demonstrating again the benefit of lower initial concentration to the refining efficiency. Therefore, it is suggested to apply the zone refining process only when an already pure Al is used as the initial material.

**Author Contributions:** B.F. was the principal investigator and final proof reader; X.Z. and S.F., conceived and designed the experiments, analyzed the data as well as wrote and edited the manuscript. All authors have read and agreed to the published version of the manuscript.

**Funding:** This research received no external funding.

**Institutional Review Board Statement:** Not applicable.

**Informed Consent Statement:** Not applicable.

**Data Availability Statement:** Not applicable.

**Acknowledgments:** The authors would like to thank CSC—China Scholarship Council for the financial support of Xiaoxin Zhang, who conducted the investigation of this work in the frame of his PhD project at IME/RWTH Aachen University.

**Conflicts of Interest:** The authors declare no conflict of interest.

## Appendix A

**Table A1.** Impurity concentration along the bar after five passes of zone refining using commercial pure Al as initial material analyzed by ICP-OES.

1.2 mm/min	Position (cm)	Fe	Si	Ga	V	Ni	Ti	Total Impurities	Al
		%	ppm	ppm	ppm	ppm	ppm	%	%
<b>Initial composition</b>		0.145	354	77	51	35	26	0.20	99.8
1st pass	2	0.16	228	95	73	34	29	0.21	99.8
	12	0.14	170	78	84	26	37	0.18	99.8
	22	0.14	209	86	74	26	30	0.18	99.8
	32	0.072	136	61	116	<10	66	0.11	99.9
	42	0.10	220	82	96	18	47	0.15	99.9
	52	0.17	370	131	72	47	29	0.23	99.8
	62	0.088	118	89	95	12	47	0.12	99.9
	72	0.14	222	65	103	30	55	0.19	99.8
	82	0.22	335	124	62	54	20	0.28	99.7
	92	0.23	479	167	57	65	14	0.31	99.7
3rd pass	2	0.13	199	81	89	30	43	0.17	99.8
	12	0.11	131	62	92	17	45	0.14	99.9
	22	0.13	143	78	81	26	36	0.17	99.8
	32	0.13	119	71	85	21	39	0.16	99.8
	42	0.15	196	89	70	32	26	0.19	99.8
	52	0.084	118	67	100	14	49	0.12	99.9
	62	0.16	251	107	56	34	13	0.21	99.8
	72	0.33	541	189	31	94	<10	0.42	99.6
	82	0.32	440	195	27	91	<10	0.40	99.6
	92	0.50	990	312	14	162	<10	0.55	99.5
5th pass	98	1.05	2500	599	15	382	<10	1.15	98.9
	2	0.095	97	55	99	13	48	0.13	99.9
	12	0.044	33	31	139	<10	88	0.07	99.9
	22	0.097	118	57	91	13	42	0.13	99.9
	32	0.069	29	47	111	<10	59	0.09	99.9
	42	0.11	106	75	82	24	35	0.14	99.9
	52	0.12	130	79	77	21	30	0.15	99.8
	62	0.17	246	112	52	39	10	0.22	99.8
	72	0.19	338	125	54	46	11	0.25	99.8
	82	0.35	538	211	28	103	<10	0.44	99.6
	92	0.38	758	256	36	126	<10	0.50	99.5
	98	0.51	1400	348	13	171	<10	0.56	99.4

**Table A2.** Impurity concentration along the bar after five passes of zone refining using recycled Al as initial material analyzed by ICP-OES.

1.2 mm/min	Position (cm)	Mg	Mn	Fe	Si	Cu	Zn	Ti	Cr	Ga	Total Impurities	Al
		%	%	%	%	%	ppm	ppm	ppm	ppm	%	%
	<b>Initial composition</b>	0.99	0.86	0.42	0.18	0.15	310	180	140	90	2.66	97.3
<b>1st pass</b>	2	0.73	0.60	0.32	0.093	0.12	403	251	197	156	1.96	98.0
	12	0.69	0.61	0.31	0.092	0.11	394	270	203	153	1.91	98.1
	22	0.74	0.62	0.34	0.095	0.12	411	212	197	159	2.01	98.0
	32	0.80	0.63	0.36	0.11	0.14	438	196	196	172	2.14	97.9
	42	0.66	0.60	0.27	0.082	0.11	375	272	202	149	1.82	98.2
	52	0.72	0.61	0.31	0.12	0.12	368	255	199	157	1.98	98.0
	62	0.69	0.60	0.28	0.10	0.11	340	277	201	151	1.88	98.1
	72	0.88	0.63	0.43	0.13	0.17	356	137	186	187	2.33	97.7
	82	0.90	0.65	0.44	0.16	0.17	325	145	189	191	2.41	97.6
	92	0.99	0.67	0.50	0.16	0.20	307	100	186	212	2.60	97.4
	98	1.19	0.70	0.66	0.15	0.27	339	35	171	256	3.05	96.9
<b>3rd pass</b>	2	0.61	0.60	0.24	0.064	0.094	339	352	204	136	1.71	98.3
	12	0.55	0.58	0.21	0.048	0.080	313	391	210	129	1.57	98.4
	22	0.54	0.58	0.20	0.047	0.080	297	405	212	129	1.55	98.4
	32	0.64	0.61	0.26	0.066	0.10	314	280	203	142	1.77	98.2
	42	0.60	0.59	0.21	0.091	0.089	277	200	199	133	1.66	98.3
	52	0.69	0.61	0.30	0.093	0.12	273	179	191	152	1.89	98.1
	62	0.72	0.63	0.33	0.11	0.12	238	131	190	158	1.98	98.0
	72	1.03	0.68	0.58	0.20	0.21	245	49	173	212	2.77	97.2
	82	1.09	0.68	0.62	0.22	0.24	220	34	169	233	2.92	97.1
	92	1.12	0.65	0.60	0.18	0.25	216	34	170	248	2.87	97.1
	98	1.27	0.68	0.72	0.20	0.31	233	15	161	283	3.25	96.8
<b>5th pass</b>	2	0.44	0.56	0.14	0.071	0.062	261	694	227	119	1.40	98.6
	12	0.50	0.58	0.17	0.089	0.070	278	417	217	122	1.51	98.5
	22	0.45	0.58	0.16	0.072	0.07	244	445	219	117	1.43	98.6
	32	0.54	0.59	0.22	0.092	0.08	255	256	204	130	1.61	98.4
	42	0.61	0.61	0.27	0.10	0.10	235	156	200	143	1.76	98.2
	52	0.65	0.62	0.30	0.094	0.11	217	126	193	151	1.84	98.2
	62	0.70	0.64	0.35	0.11	0.12	208	79	190	163	1.98	98.0
	72	0.84	0.68	0.46	0.16	0.16	195	63	185	188	2.36	97.6
	82	1.10	0.66	0.63	0.23	0.25	202	18	164	245	2.93	97.1
	92	1.19	0.64	0.64	0.22	0.28	201	15	158	267	3.03	97.0
	98	1.35	0.61	0.71	0.20	0.34	217	<5	149	306	3.28	96.7

## References

1. Curtolo, D.; Friedrich, S.; Bellin, D.; Nayak, G.; Friedrich, B. Definition of a First Process Window for Purification of aluminum via “Cooled Finger” Crystallization Technique. *Metals* **2017**, *7*, 341. [[CrossRef](#)]
2. Pearce, J.V. Distribution coefficients of impurities in metals. *Int. J. Thermophys.* **2014**, *35*, 628–635. [[CrossRef](#)]
3. Huntley, D.A.; Shah, J.S. High resistance ratio antimony. *J. Cryst. Growth* **1970**, *6*, 216–218. [[CrossRef](#)]
4. Hashimoto, E.; Ueda, Y. Zone Refining of high-purity aluminum. *Mater. Trans.* **1994**, *35*, 262–265. [[CrossRef](#)]
5. Munirathnam, N.R.; Prasad, D.S.; Sudheer, C.; Prakash, T.L. Purification of tellurium to 6N + by quadruple zone refining. *J. Cryst. Growth* **2003**, *254*, 262–266. [[CrossRef](#)]
6. Munirathnam, N.R.; Prasad, D.S.; Sudheer, C.H.; Rao, J.V.; Prakash, T.L. Zone refining of cadmium and related characterization. *Bull. Mater. Sci.* **2005**, *28*, 209–212. [[CrossRef](#)]
7. Yang, G.; Guan, Y.T.; Jian, F.Y.; Wagner, M.D.; Mei, H.; Wang, G.J.; Howard, S.M.; Mei, D.M.; Nelson, A.; Marshal, J.; et al. Zone Refinement of Germanium Crystals. *J. Phys. Conf. Ser.* **2015**, *606*, 012014. [[CrossRef](#)]
8. Pfann, W.G. Principles of zone melting. *Trans. AIME* **1952**, *194*, 747. [[CrossRef](#)]
9. Viggdorovich, V.N. *Purification of Metals and Semiconductors by Crystallization*; Freund Publishing House: Moscow, Russia, 1969.
10. Ghosh, K.; Mani, V.N.; Dhar, S. A modeling approach for the purification of group III metals (Ga and In) by zone refining. *J. Appl. Phys.* **2008**, *104*. [[CrossRef](#)]

11. Ghosh, K.; Mani, V.N.; Dhar, S. Numerical study and experimental investigation of zone refining in ultra-high purification of gallium and its use in the growth of GaAs epitaxial layers. *J. Cryst. Growth* **2009**, *311*, 1521–1528. [[CrossRef](#)]
12. Kino, T.; Kamigaki, N.; Yamasaki, H.; Kawai, J.; Deguchi, Y.; Nakamichi, I. Zone Refining in aluminum. *Trans. Jpn. Inst. Met.* **1976**, *17*, 645–648. [[CrossRef](#)]
13. Nakamura, M.; Watanabe, M.; Tanaka, K.; Kirihata, A.; Sumomogi, T.; Hiroaki, H.; Tanaka, I. Zone Refining of aluminum and its Simulation. *Mater. Trans.* **2014**, *55*, 664–670. [[CrossRef](#)]
14. Yang, G.; Govani, J.; Mei, H.; Guan, Y.; Wang, G.; Huang, M.; Mei, D. Investigation of influential factors on the purification of zone-refined germanium ingot. *Cryst. Res. Technol.* **2014**, *49*, 269–275. [[CrossRef](#)]
15. Munirathnam, N.R.; Prasad, D.S.; Sudheer, C.; Singh, A.J.; Prakash, T.L. Preparation of high purity tellurium by zone refining. *Bull. Mater. Sci.* **2002**, *25*, 79–83. [[CrossRef](#)]
16. Curtolo, D.; Zhang, X.; Rojas, M.; Friedrich, S.; Friedrich, B. Realization of the Zone Length Measurement during Zone Refining Process via Implementation of an Infrared Camera. *Appl. Sci.* **2018**, *8*, 875. [[CrossRef](#)]
17. Spim, J.A.; Bernadou, M.J.S.; Garcia, A. Numerical modeling and optimization of zone refining. *J. Alloy. Compd.* **2000**, *298*, 299–305. [[CrossRef](#)]
18. Leslie Burris, J.; Stockman, C.H.; Dillon, I.G. Contribution to mathematics of zone refining. *J. Miner. Met. Mater. Soc.* **1955**, *7*, 1017–1023. [[CrossRef](#)]
19. Pfann, W.G. *Zone Melting*, 2nd ed.; John Wiley and Sons Inc.: New York, NY, USA, 1966.
20. Ho, C.; Yeh, H.; Yeh, T. Numerical analysis on optimal zone lengths for each pass in multipass zone-refining processes. *Can. J. Chem. Eng.* **1998**, *76*, 3–9. [[CrossRef](#)]
21. Rodway, G.H.; Hunt, J.D. Optimizing zone refining. *J. Cryst. Growth* **1989**, *97*, 680–688. [[CrossRef](#)]
22. Zhang, X.; Friedrich, S.; Friedrich, B. Characterization and interpretation of the aluminum zone refining through infrared thermographic analysis. *Materials* **2018**, *11*, 2039. [[CrossRef](#)] [[PubMed](#)]